ELSEVIER

Biochimica et Biophysica Acta 1365 (1998) 404–420

BIOCHIMICA ET BIOPHYSICA ACTA
BBA

Triplet energy transfer in bacterial photosynthetic reaction centres

A. Angerhofer [a,b,*], F. Bornhäuser [b], V. Aust [b,c], G. Hartwich [d,e], H. Scheer [f]

[a] *Department of Chemistry, University of Florida, Gainesville, FL 32611, USA*
[b] *3. Physikalisches Institut, Universität Stuttgart, D-70550 Stuttgart, Germany*
[c] *Ernst Mach Institut, Hauptstr. 18, D-79576 Weil a. Rhein, Germany*
[d] *Institut für Physikalische und Theoretische Chemie, Lichtenbergstr. 4, Technische Universität München, D-85747 Garching, Germany*
[e] *Department of Chemical Engineering, University of Texas at Austin, Austin, TX 78712-1062, USA*
[f] *Botanisches Institut, Universität München, Menzinger Str. 67, D-80638 Munich, Germany*

Received 20 February 1998; accepted 2 April 1998

Abstract

[3-vinyl]-13^2-OH-bacteriochlorophyll *a* has been selectively exchanged against native bacteriochlorophyll *a* in the monomer binding sites at the A- and B-branch of the photosynthetic reaction centre from *Rhodobacter sphaeroides*. Transient absorption difference measurements were performed on these samples over a temperature range from 4.2 to 300 K with 20 ns time resolution. Specifically the decay of the primary donor triplet state, $^3P_{870}$, as well as the rise and decay rates of the carotenoid triplet state, ^{3}Car (spheroidene), were measured. The observed rates revealed a thermally activated carotenoid triplet formation corresponding to the decay of the primary donor triplet state. The activation energies for the triplet energy transfer process were 100($\pm$10) cm^{-1} for reaction centers from wild-type *Rhodobacter sphaeroides* 2.4.1, with and without exchange of the monomeric bacteriochlorophyll on the electron transfer-active branch, B_A. For reaction centers from *Rhodobacter sphaeroides* R26.1 with both monomers exchanged against [3-vinyl]-13^2-OH-bacteriochlorophyll *a*, and subsequent spheroidene reconstitution the activation energy was 460($\pm$20) cm^{-1}. These activation energies correspond to the energy difference between the triplet states of the accessory BChl monomer, B_B, and the primary donor when native BChl *a* or [3-vinyl]-13^2-OH-BChl *a* is present in the B_B binding site. In all samples the ^{3}Car formation rates were bi-phasic over a large temperature range. A fast temperature-independent rate was observed on the wavelength of the carotenoid triplet–triplet absorption which dominated at very low temperatures. Additionally, a slower temperature-independent ^{3}Car formation rate was observed at low temperatures which could be explained with the assumption of heterogeneity in the energy barrier (^3B_B) and/or the primary donor triplet state ($^3P_{870}$). A tunneling mechanism as proposed earlier by Kolaczkowski (PhD thesis, Brown University, 1989) is not only unnecessary but also incompatible with the available experimental data.

Keywords: Photosynthesis; Reaction centre; Pigment modification; Triplet state; Transient absorption; (*Rhodobacter sphaeroides*)

Abbreviations: ADMR, absorption detected magnetic resonance; $B_{A,B}$, accessory monomers on A- and B-branch; BChl, bacteriochlorophyll; BPh, bacteriopheophytin; Car, carotenoid; DAD-HPLC, diode-array detected high performance liquid chromatography; DEAE, diethylaminoethylcellulose; LD-ADMR, linear dichroism detected ADMR; LDAO, lauryldimethylamine oxide; LD-MIA, linear dichroism detected MIA; MIA, microwave induced absorption; MODS, magneto-optical difference spectroscopy; P_{870}, primary donor 'special pair'; RC, reaction centre; TL-buffer, 10 mM Tris-hydroxymethylaminomethane hydrochloride, pH 8, containing 0.08% LDAO; T-S, triplet-minus-singlet

* Corresponding author. Fax: +1 (352) 392 0872; E-mail: alex@chem.ufl.edu

0005-2728/98/$19.00
PII: S0005-2728(98)00093-0

1. Introduction

Reaction centres (RC) of the purple photosynthetic bacterium *Rhodobacter* (*Rb.*) *sphaeroides* 2.4.1 contain four bacteriochlorophyll *a* (BChl *a*), two bacteriopheophytin *a* (BPh *a*), two ubiquinone-10, and one spheroidene molecule [2–4] in a protein complex comprised of 3 polypeptides traditionally labeled L, M, and H [5,6]. Their molecular structure has been revealed by single crystal X-ray crystallography [7–9].

One of the main roles of carotenoids in photosynthetic pigment–protein complexes is photo-protection [10,11]. In order to prevent harmful radicals or singlet oxygen to be sensitized by chlorophyll triplet states the latter are quickly quenched by the carotenoids. While chlorophyll triplet states are not involved in the primary processes of photosynthesis they can accidentally form under high light flux conditions. In the case of plant photosystem II they are probably involved in photo-inhibition, a process by which photosynthetic production is decreased under high light irradiation [12].

The question of triplet energy transfer in the bacterial reaction center, and hence the question of the photo-protective role of its carotenoid composition, has been discussed in the literature for the last twenty years.

Cogdell and co-workers first showed that the triplet state of the primary donor $^3P_{870}$, termed P^R, was efficiently quenched producing a triplet excited carotenoid [13,14]. In fact, the primary donor triplet was not observed at all in the wild-type RCs, and the time of formation of ^{3}Car was of the order of tens of nanoseconds depending on temperature.

A temperature dependent study of the decay rate of $^3P_{870}$ and quantum yield of ^{3}Car demonstrated the existence of a triplet excited intermediate state which was thermally accessible from $^3P_{870}$ [15]. At first it was tentatively assigned to a triplet charge transfer (CT) state, $^3[P^+_{870}B^-]$, to be formed between the primary donor and one of the BChl monomers [15,16]. However, the admixture of such a CT state to the $^3P_{870}$ state was later rejected based on the temperature dependent investigation of the triplet fine structure splitting with EPR and MODS spectroscopies [17,18]. Instead, a temperature dependent admixture of the triplet state of the monomeric BChl on the electron transfer-inactive side of the RC was proposed to account for the increase in the fine structure parameter $|D|$ [19]. Temperature-dependent absorption detected magnetic resonance (ADMR) of $^3P_{870}$ and the theoretical calculation of the fine structure parameters based on the X-ray structure later proved that admixture of ^3B_B to $^3P_{870}$ is unable to explain the temperature dependence of $|D|$ and $|E|$ [20,21]. While these experiments did not exclude B_B from acting as the bridge for triplet energy transfer they pointed to the need for further investigation of the existence and role of low energy excitations between 100 and 200 cm^{-1} above the first excited triplet zero-phonon level. Further indication for such a nearby triplet state that may be located on the primary donor came from time-resolved zero field ADMR experiments [22].

The hypothesis that ^3B_B actually is an intermediate state in triplet energy transfer from $^3P_{870}$ [19] gained strong support from the phosphorescence data on BChl and bacterial RCs by Takiff and Boxer [23,24]. They estimated the triplet energy level of the monomeric BChl, ^3B_B, 200 cm^{-1} above that of $^3P_{870}$, at most [24], right in the range where the transient intermediate state was supposed to be according to Schenck et al. [15]. This hypothesis was further strengthened by Frank and co-workers who studied borohydride-treated RCs by transient absorption and temperature dependent EPR [25,26]. They came to the conclusion that B_B is essential to triplet energy transfer from $^3P_{870}$ to Car. This was further corroborated by the observation of different temperatures of onset of ^{3}Car formation in RCs from *Rb. sphaeroides*, where the triplet energy level of ^3B_B was changed by exchanging the corresponding pigment against structural analogs [27]. In these preparations, B_B was exchanged against (1) [3-vinyl]-13^2-OH-BChl *a*, and (2) 13^2-OH-Zn-BPh *a* which feature blue-shifted $S_0 \rightarrow S_1$ transitions compared to native BChl *a* and probably similarly higher triplet energy levels. Correspondingly, the ^{3}Car EPR signals started to appear at different temperatures due to the different energy barriers presented by the exchanged pigments. The energetic position of the triplet states of the intermediate B_B in native and modified RCs has been determined by Frank et al. [28] through analysis of the temperature dependence of the formation rate of ^{3}Car.

Although the picture of B_B serving as the bridge for triplet energy transfer between P_{870} and Car and the mounting evidence for it seems very convincing, this simple model cannot account for the following experimental observations: (1) Kolaczkowski found a biphasic ^{3}Car formation process below approx. 150 K which he interpreted as due to direct low temperature tunneling of the triplet excitation from $^3P_{870}$ to ^{3}Car, as well as a fast temperature-independent triplet energy transfer from $^3[P^+_{870}H^-]$ to ^{3}Car bypassing $^3P_{870}$ [1]. (2) Zero field ADMR experiments showed the presence of ^{3}Car at temperatures well below the point where the thermally activated process is shut off [29–31], indicating a possible alternate triplet energy transfer pathway.

In the present paper we report on transient absorption spectra designed to clear up some of the yet open questions about triplet energy transfer in the bacterial photosynthetic RC of *Rb. sphaeroides*. Our aims were: (1) to revisit the older data of Schenck et al. [15] and Kolaczkowski [1] by detecting both $^3P_{870}$ decay and ^{3}Car formation at the same time, and (2) to extend these investigations to RCs where the BChl monomers had been exchanged against [3-vinyl]-13^2-OH-BChl *a* in order to distinguish between kinetic components due to the thermally activated pathway $^3P_{870} \rightarrow {}^3B_B \rightarrow {}^3$Car and possible other contributions.

2. Materials and methods

2.1. Sample preparation

Reaction centres of *Rb. sphaeroides* R26.1 and wild-type strain 2.4.1 were isolated as described elsewhere [32–34]. [3-vinyl]-13^2-OH-BChl *a* was prepared from BChl *a* by reduction of the 3-acetyl group with $NaBH_4$ to 3-α-OH-ethyl and subsequent dehydration in pyridine to [3-vinyl]-BChl *a*. Hydroxylation at the 13^2-position occurs when [3-vinyl]-BChl is dissolved in methanol and kept in the dark for several days at 4°C in the presence of air [35].

Simultaneous exchange of BChl at the sites B_A and B_B against [3-vinyl]-13^2-OH-BChl *a* is possible by treating R26.1 RCs (OD/cm = 1 at 865 nm), dissolved in TL-buffer (10 mM Tris, 0.08% lauryldimethylamine oxide (LDAO), at pH 8) with a tenfold molar excess of [3-vinyl]-13^2-OH-BChl *a* in methanolic solution for 90 min at 43°C. The organic solvent should not exceed 10% of the whole reaction volume in order to avoid extensive loss of RCs during the treatment by irreversible denaturation. Purification of exchanged RCs from extra pigment and denatured protein is done on DEAE-cellulose. The overall exchange rate was determined by pigment extraction and subsequent diode-array detected high performance liquid chromatography (DAD-HPLC) [36,37]. Repeating the whole exchange experiment one or two times leads to nearly quantitative replacement of native monomeric BChl. In the actual $B_{A,B}$-exchanged sample approx. 95 ± 3% of the native monomeric BChl is replaced [38].

For introduction of spheroidene in carotenoid-less RC, it is dissolved to maximum concentration in diethyl ether and then diluted with 3 parts (v/v) methanol. This mixture was added to the RCs (OD/cm = 1 at 865 nm) to a final concentration of organic solvent of 10%. The reaction time is only 50 min at 43°C, by which about 90% of the RCs are reconstituted with the carotenoid (according to DAD-HPLC analysis). In the $B_{A,B}$-exchanged sample spheroidene is reconstituted to 93% (compared to the wild-type 2.4.1 RCs, and estimated from room temperature integral absorption at 505 nm relative to the integral primary donor absorption at 865 nm).

Selective BChl exchange at the B_A-site only is achieved in wild-type RCs of the strain 2.4.1. They naturally contain spheroidene close to the B_B monomer which blocks the exchange there. The exchange rate of the B_A-exchanged sample is approx. 47% of the monomeric BChl, corresponding to 94% replacement at B_A. The carotenoid content is 98%.

All RC preparations with exchanged pigments show the normal primary donor bleaching when exposed to actinic light. The CD spectra show no detectable structural changes besides spectral shifts due to the different absorption bands of the exchanged pigments [38].

2.2. Spectroscopic methods

Our set-up for transient optical spectroscopy has been described previously [39]. Briefly, an excimer-pumped dye laser is used for pulsed excitation (Lambda Physik LPX240iCC pumping LPD 3002)

using styryl 9. The excitation wavelength could be varied between 820 and 860 nm and was adjusted to give optimum excitation in the NIR (around 850 nm even at lower temperatures due to the drop-off in dye performance). Pulse widths are slightly shorter than 20 ns with the energy per pulse set to approximately 1 mJ, spread over approx. 6 mm^2 of sample area to avoid saturation. Detection light was provided by a tungsten-halogen lamp using appropriate filter combinations for the visible and NIR detection bands. We used a blue-enhanced silicon avalanche photodiode with a bandwidth of 250 MHz (Hamamatsu, model S5343) for detection of the laser-induced transmission changes. It was situated in a double Faraday cage to avoid electromagnetic interference from the firing of the laser thyratron. Data acquisition and averaging was performed by a LeCroy 9400 digital oscilloscope.

2.3. Theoretical description of the 4-state model

In order to describe the triplet energy transfer in the photosynthetic RC we used a 4-state model, as shown in Fig. 1. We call it a 4-state model because the 4 excited and 3 ground states can be approximated by a system of 4 linear inhomogeneous differential equations, describing the dynamics of the 4-excited states. It includes the primary radical pair triplet state, $^3[P^+_{870}H^-]$ as the first step of triplet generation. All precursor states to $^3[P^+_{870}H^-]$ are implicitly included in the excitation rate $k_{1\leftarrow0}$ which leads to the population of state 1 from the ground state (state 0). $k_{0\leftarrow1}$ describes the decay of $^3[P^+_{870}H^-]$ back to the ground state via spin-flip to $^1[P^+_{870}H^-]$ and charge recombination. $k_{2\leftarrow1}$ describes the electron-hole recombination into the primary donor triplet state $^3P_{870}$ (state 2), and $k_{1\leftarrow2}$ the thermally activated charge separation from $^3P_{870}$ to $^3[P^+_{870}H^-]$. $k_{0\leftarrow2}$ is the rate of molecular intersystem crossing (ISC) within the primary donor which leads to radiation-less deactivation of $^3P_{870}$. $k_{3\leftarrow2}$ describes the thermally activated population of the monomeric triplet state ^3B_B (state 3), $k_{2\leftarrow3}$ its reverse reaction. The quenching of ^3B_B by the carotenoid is described by $k_{4\leftarrow3}$ with $k_{3\leftarrow4}$ as its thermally activated reverse process. $k_{6\leftarrow4}$ finally describes the ISC and relaxation of ^{3}Car (state 4) back to the ground state of the complex. Relaxation of ^3B_B via ISC is not considered since triplet energy transfer to ^{3}Car is expected to be much faster. In order to accommodate the hypothesis of tunneling between $^3P_{870}$ and ^{3}Car and the notion that the thermalized $^3P_{870}$ may be bypassed in the quenching reaction, as put forward by Kolaczkowski [1], we also consider the rates $k_{3\leftarrow1}$ and $k_{4\leftarrow2}$ as potential triplet energy transfer pathways. Their arrows appear dotted to denote their speculative nature. We can show in our analysis that these processes are not necessary to explain the available experimental data.

The details of the mathematical description of the model have been presented in [40].

In order to analyze the predictions of these different models and to compare them with the experimental data we need to define the reaction rates in the model. These rates greatly depend on the mechanisms that underly the respective reactions. We use literature values for $k_{i\leftarrow j}$ and their temperature dependencies wherever they are available, in order to leave the least number of free parameters for the comparison between model and data.

2.3.1. Excitation

The excitation rate, $k_{1\leftarrow0}$, depends largely on the experimental parameters. In our case, under cw illumination of the detection lamp a maximum of 2000 s^{-1} can be achieved with full sample illumination with the white light filtered only through a 3-cm layer of water [22,41]. Since we used the normal ADMR excitation channel only for the probing light the level of excitation was reduced by interference filters and reduction of the lamp current to yield approx. $k_{1\leftarrow0} = 100\cdots200\ s^{-1}$. For the modeling of the kinetic experiment a non-saturating flash was assumed, i.e., a $^3[P^+_{870}H^-] : [P]$ (triplet radical pair/ground state) ratio of less than 5% was used as the initial starting condition.

2.3.2. $^3[P^+_{870}H^-]$ decay

The transient decay of $^1[P^+_{870}H^-]$ and $^3[P^+_{870}H^-]$ has been studied extensively in the literature. While it is not possible to distinguish between the two states by purely optical means their rates can be obtained by analyzing the magnetic field and RYDMR effects on the $^3P_{870}$ yield and lifetime [1,42–49]. $k_{2\leftarrow1}$ is identified with the rate of charge recombination of $^3[P^+_{870}H^-]$ into the molecular triplet state of the pri-

mary donor. It is of the order of $3\cdots6\times10^8$ s^{-1} [43,46–48] and depends very little on temperature since the energy gap between $^3[P^+_{870}H^-]$ and $^3P_{870}$ ($\sim1370\pm30$ cm^{-1} [50,51]) approximately equals its reorganization energy [52,53]. We take $k_{2\leftarrow1}=4\times10^8$ s^{-1} from Goldstein and Boxer [48] and leave it temperature independent for our model calculations.

$k_{0\leftarrow1}$ has to be identified with the back reaction of $^3[P^+_{870}H^-]$ into the ground state. This involves a hyperfine-mediated spin flip to get to the practically isoenergetic singlet radical pair, $^1[P^+_{870}H^-]$, and consecutive recombination into the ground state. This reaction lies deep in the Marcus inverted range which makes it thermally activated ($2\cdots4\times10^7$ s^{-1} between 80 and 300 K) [53]. We approximate the literature values [43,46] with the following temperature dependent function

$$k_{0\leftarrow1}=\left\{1.3\times10^7+2\times10^8\times\exp\left(\frac{-440[\mathrm{K}]}{T}\right)\right\}\mathrm{s}^{-1} \quad (1)$$

$k_{3\leftarrow1}$ describes a potential bypass reaction by which the radical pair triplet state decays directly into ^3B_B bypassing the vibronically relaxed $^3P_{870}$. It is similar to the model proposed by Kolaczkowski to account for the fast population kinetics of the carotenoid triplet [1]. It can be switched on in our model calculations by assigning it a rate that is competitive with the $^3[P^+_{870}H^-]$ decay.

2.3.3. $^3P_{870}$ decay

$k_{0\leftarrow2}$ is the molecular intersystem-crossing (ISC) decay rate of the primary donor triplet $^3P_{870}$. It is almost temperature independent at around $6\cdots8\times10^3$ s^{-1} [43,45].

On the other hand, the observed $^3P_{870}$ decay rate in carotenoid-free *Rb. sphaeroides* R26.1 appears thermally activated above approx. 160 K with activation energies between 750 and 950 cm^{-1} [43,45,54]. This activation energy does not seem to reflect the free energy drop between $^3[P^+_{870}H^-]$ and $^3P_{870}$ which is somewhat larger (0.13 eV) [43,50,51]. The cause for this thermal activation still seems to be unresolved at least for quinone-reduced RCs [43]. For our simulation purposes we take

$$k_{1\leftarrow2}=k_{2\leftarrow1}\times\exp\left\{\frac{-\Delta G_{(^3[P^+_{870}H^-]-^3P_{870})}}{k_BT}\right\} \quad (2)$$

with $-\Delta G_{(^3[P^+_{870}H^-]-^3P_{870})}$=0.13 eV from [43].

2.3.4. ^3B_B population and decay

In principle triplet energy transfer to B_B can be described by the Marcus theory as Closs and coworkers demonstrated for model systems [55].

The apparent rates $k_{2\leftarrow3}$ and $k_{4\leftarrow3}$ which describe the decay of ^3B_B can be assumed to be of the order of 1×10^9 s^{-1} or larger since otherwise the intermediate ^3B_B should show up as a separate kinetic component in our and others' transient absorption experiments. The back reaction rates, $k_{3\leftarrow2}$ and $k_{3\leftarrow4}$ are related to the forward rates by their corresponding Boltzmann factors $\exp\{-\Delta G_{(^3B_B-^3P_{870})}/k_BT\}$ and $\exp\{-\Delta G_{(^3B_B-^3Car)}/k_BT\}$, i.e.,

$$k_{3\leftarrow2}=k_{2\leftarrow3}\times\exp\left\{-\frac{\Delta G_{(^3B_B-^3P_{870})}}{k_BT}\right\} \quad (3)$$

and

$$k_{3\leftarrow4}=k_{4\leftarrow3}\times\exp\left\{-\frac{-\Delta G_{(^3B_B-^3Car)}}{k_BT}\right\} \quad (4)$$

The purported tunneling rate $k_{4\leftarrow2}$ is assumed to be temperature independent, and of the order of 1×10^6 s^{-1} in order to be meaningful as a separate triplet transfer mechanism at low temperatures.

2.3.5. ^3Car decay

^{3}Car decays via ISC. It is only slightly temperature

Table 1
Sample preparations used in this study

Sample	B_A	B_B	Carotenoid
A	BChl *a*	BChl *a*	Native
B	Vinyl-BChl *a*	BChl *a*	Native
C	Vinyl-BChl *a*	Vinyl-BChl *a*	Reconstituted

The carotenoid present is always spheroidene, either naturally by using the wild-type strain or by reconstitution into the mutant strain R26.1. Vinyl-BChl *a* stands short for [3-vinyl]-13^2-OH-BChl *a*.

dependent and stays within $1\cdots2\times10^5$ s^{-1} (from ^{3}Car decay, data not shown).

3. Results

Transients were investigated on the ^{3}Car triplet–triplet absorption band of spheroidene (550 nm) and the P_{870} singlet–singlet absorption band (870–895 nm, depending on temperature). In order to observe and correctly analyze the rise and decay of the various transients different time bases were used on the digitizing oscilloscope to cover different kinetic components. Three different samples were used with different degrees of BChl monomer exchange as indicated in Table 1, and spheroidene as the carotenoid.

Fig. 2 shows some of the typical transients obtained at 550 and 895 nm and their respective mono- and bi-exponential fits. As it turns out, many of the transients had to be fitted bi-exponentially over a large temperature range in order to obtain satisfactory fits.

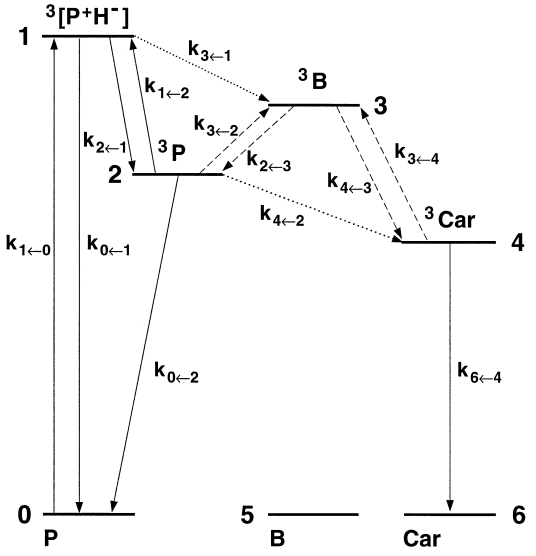

Fig. 1. The 4-state model used for the description of triplet energy transfer in the RC. For detailed explanation, see text. The filled arrows denote the rates that have been observed and described in the literature. The broken arrows depict rates that are unknown (from and to ^3B_B), the dotted ones show rates that are speculative ($k_{3\leftarrow1}$ for bypass reaction, and $k_{4\leftarrow2}$ for tunneling). The rates defined by arrows between different molecules (P, B, and Car) are in reality second order rates, i.e. they depend on the ground state concentrations of the molecule the excited state of which they point to.

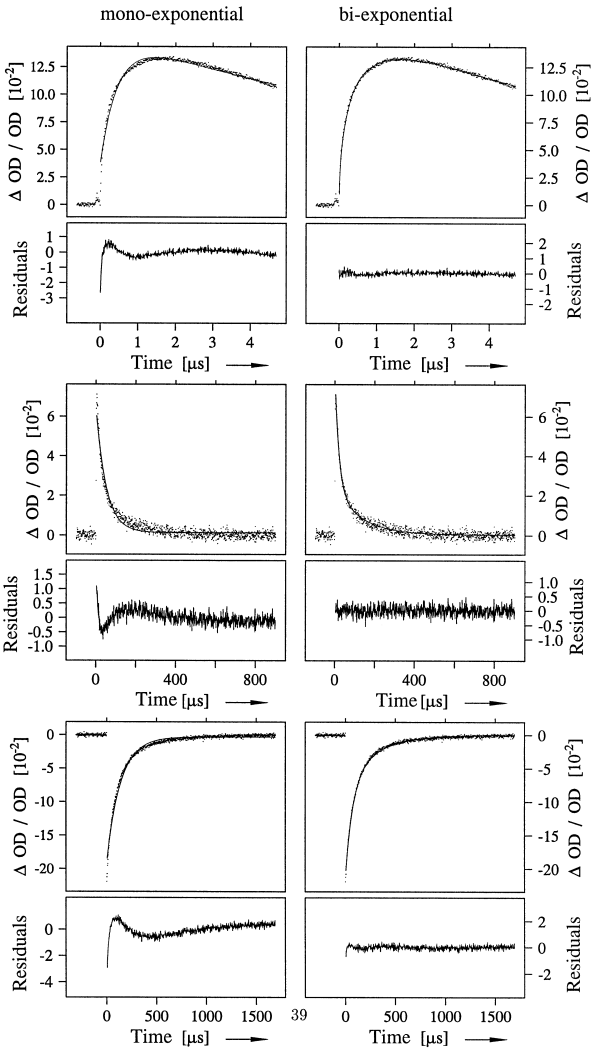

Fig. 2. Comparison of mono- and bi-exponential fits to the rise (upper traces, at 45 K) and decay (middle traces, at 30 K) of the transient triplet–triplet absorption of ^{3}Car observed at 550 nm, and the decay (lower traces, at 35 K) of $^3P_{870}$ observed at 895 nm. Excitation by a 20-ns wide laser pulse at 855 nm. The transients were taken with sample A (*Rb. sphaeroides* 2.4.1).

3.1. Fast transients observed at 550 nm (^{3}Car triplet–triplet absorption)

In order to correctly fit the rate of ^{3}Car formation (see for example Fig. 2, upper traces) its decay rate has to be used in the simulation function. It was derived from the ^{3}Car decay analyzed from transients obtained on a longer time scale (e.g., Fig. 2, middle traces), and was included as a fixed parameter in the fit of the multi-exponential rise and decay curves obtained on a short time scale.

These results were obtained for *Rb. sphaeroides* 2.4.1 (sample A) by the following procedure.

Below 85 K two distinct rates were necessary to obtain a good fit for the ^{3}Car formation process. Both were fairly temperature-independent below about 50 K (see Fig. 3) at around 10^{-6} and 10^{-7} s, and agree very well with previous measurements [1,28,56]. Above 85 K a mono-exponential fit was able to describe the data. It was temperature dependent with an increase in ^{3}Car-formation rate of approx. a factor of 4 between 80 and 300 K. Below 45 K the ^{3}Car absorption became so weak that the transient response of the primary donor triplet–triplet absorption (see Fig. 8) had to be taken into account and subtracted from the trace before fitting. Another effect of the low intensity of the ^{3}Car signal at low temperatures was that below about 20 K the signal-to-noise ratio became so poor that we were not able to distinguish the two rates any more, i.e., a mono-exponential fit was sufficient to describe the data (not shown).

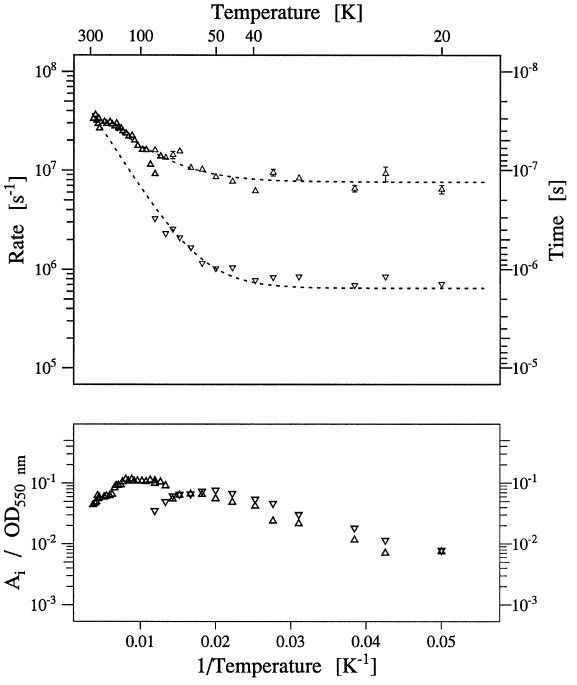

Fig. 3. Top: ^{3}Car formation rates in *Rb. sphaeroides* 2.4.1 (sample A) in an Arrhenius plot. The transients were observed at 550 nm and evaluated by either a mono- (△, $T>85$ K) or a bi-exponential (▽, $T<85$ K) fit to the rise of the signal. The dashed lines represent fits to Eq. 6 (see Table 2). Bottom: Amplitudes of the kinetic components normalized to the OD at the wavelength of observation (550 nm) with corresponding symbols. The amplitudes of the two components can be directly compared and allow to distinguish between the dominant and the minor contributions.

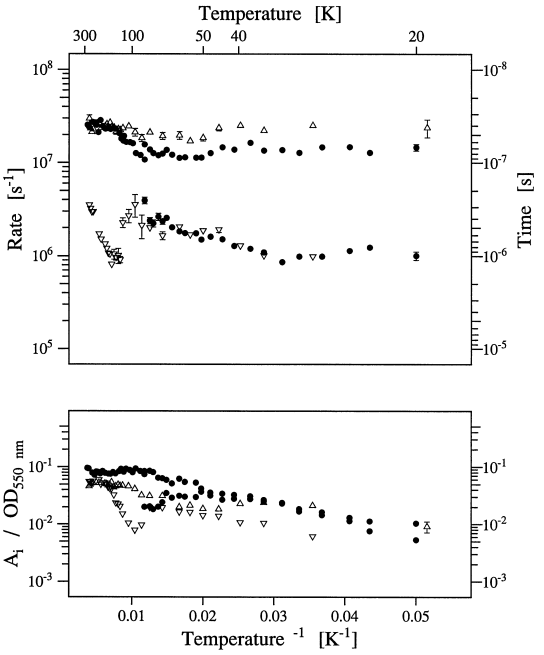

Fig. 4. Top: ^{3}Car formation rates in *Rb. sphaeroides* 2.4.1, B_A exchanged with [3-vinyl]-13^2-OH-BChl *a* (sample B, ●) and *Rb. sphaeroides* R26.1, B_A and B_B exchanged with [3-vinyl]-13^2-OH-BChl *a* and reconstituted with spheroidene (sample C, △ and ▽) in an Arrhenius plot. The transients were observed at 550 nm and evaluated by either a mono- or a bi-exponential (below 85 K for sample B, and in the whole temperature range for sample C) fit to the rise of the signal. Bottom: Amplitudes of the kinetic components normalized to the OD at the wavelength of observation (550 nm) with corresponding symbols.

Similar limitations were present in samples B and C (*Rb. sphaeroides* 2.4.1 with B_A exchanged, and *Rb. sphaeroides* R26.1 with both B_A and B_B exchanged for [3-vinyl]-13^2-OH-BChl *a*, then reconstituted with spheroidene). Fig. 4 presents the temperature dependence of the rates and amplitudes of the different components in ^{3}Car formation in samples B and C. Sample B behaved very similar to sample A. This was expected since only B_A was exchanged, but not B_B over which the triplet energy transfer process should proceed. For sample C (both BChls exchanged with [3-vinyl]-13^2-OH-BChl *a*, and reconstituted with spheroidene) we found bi-exponential ^{3}Car formation behavior in the complete temperature range above 20 K.

The most striking difference between the B_B-modi-

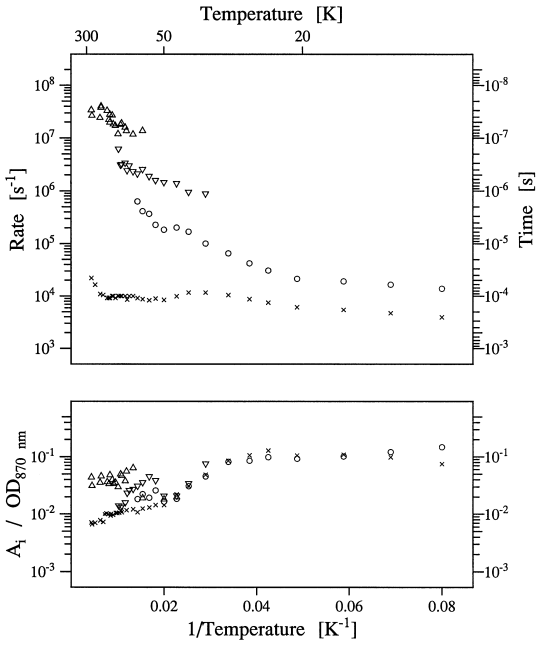

Fig. 5. Top: $^3P_{870}$ decay rates in *Rb. sphaeroides* 2.4.1 (sample A) in an Arrhenius plot. The transients were observed between 870 and 895 nm (depending on the location of the P_{870} maximum at different temperatures) in different time intervals and globally evaluated by either bi-, tri-, or tetra-exponential fits to the decay of the signal. Bottom: Amplitudes of the kinetic components normalized to the OD at the acquisition wavelength (between 870 and 895 nm) with corresponding symbols.

fied sample C and samples A and B (with native BChl at B_B) is the additional slow component in sample C which appears between 110 and 300 K. In the representation in Fig. 4 this appears as a dip in the slow rate between 110 and 300 K. A similar behavior, albeit with less data points at higher temperatures, was observed by Frank et al. in the same sample [28]. Upon raising the temperature this thermally activated component quickly gains strength surpassing the amplitude of the ever present fast component around 150 K. It thus seems to be a direct result of the exchange of B_B with [3-vinyl]-13^2-OH-BChl *a*. Except for this additional dip in the slower rate the observed rates and corresponding amplitudes are roughly the same in all three samples.

3.2. Decay rates observed on the P_{870} absorption band

The temperature dependence of the decay rates of the primary donor triplet of samples A and B (wild-type with and without B_A exchanged) are shown in Figs. 5 and 6. The main features are very similar in both samples, as expected. Below 35 K the decay is bi-exponential in sample A with both rates slowly dropping with temperature to 1.4×10^4 and 3.5×10^3 s^{-1} below 15 K due to the different triplet sublevel decay paths [22,57]. In the same temperature range, sample B exhibits a similar behavior with its sublevel decay rates at 9×10^3 and 1.5×10^3 s^{-1} and two additional faster temperature-independent decay rates at 1.2×10^6 (filled $\triangledown$) and 1.4×10^7 s^{-1} (filled $\triangle$) with weak contributions to the overall amplitude. These two additional rates merge with the temperature-dependent rate (filled $\bigcirc$) at around 60 and 90 K. Sample A shows only very weak indications of the presence of these rates setting on at higher temperatures (empty $\triangledown$ and $\triangle$). Both samples show a further slow rate of 9×10^3 s^{-1} ($\times$) at temperatures between 30 and 160 K (sample A), and between 30 and 65 K (sample B). At these temperatures the rate starts to increase linearly with decreasing inverse

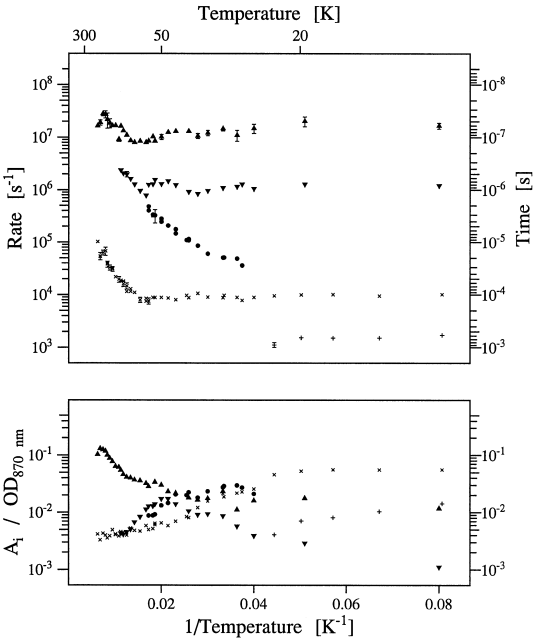

Fig. 6. Top: $^3P_{870}$ decay rates in *Rb. sphaeroides* 2.4.1, B_A exchanged with [3-vinyl]-13^2-OH-BChl *a* (sample B) in an Arrhenius plot. The transients were observed between 870 and 895 nm (depending on the location of the P_{870} maximum at different temperatures) in different time intervals and globally evaluated by either bi-, tri-, or tetra-exponential fits to the decay of the signal. Bottom: Amplitudes of the kinetic components normalized to the OD at the acquisition wavelength (between 870 and 895 nm) with corresponding symbols.

temperature. The behavior of the slow rate of sample A around 9×10^3 s^{-1} is identical with that observed in RCs of *Rb. sphaeroides* R26.1 where a thermal activation of 730 cm^{-1} had been determined for the back-reaction to $^3[P^+_{870}H^-]$ [54,56] and thus is attributed to RCs which lost their carotenoid during preparation. The amplitude of the slow rate is very weak in both samples which underlines this interpretation.

Sample C (both BChl monomers exchanged against [3-vinyl]-13^2-OH-BChl *a* and reconstituted with spheroidene) shows a drastically different behavior (see Fig. 7). While the slow component arising from the minor contribution of carotenoid-free RCs is again present (at 9×10^3 s^{-1} with an additional component at 2.3×10^3 s^{-1} below 25 K, and a thermally activated behavior above 160 K (×)), there is only one additional, thermally activated decay rate visible above 90 K (○).

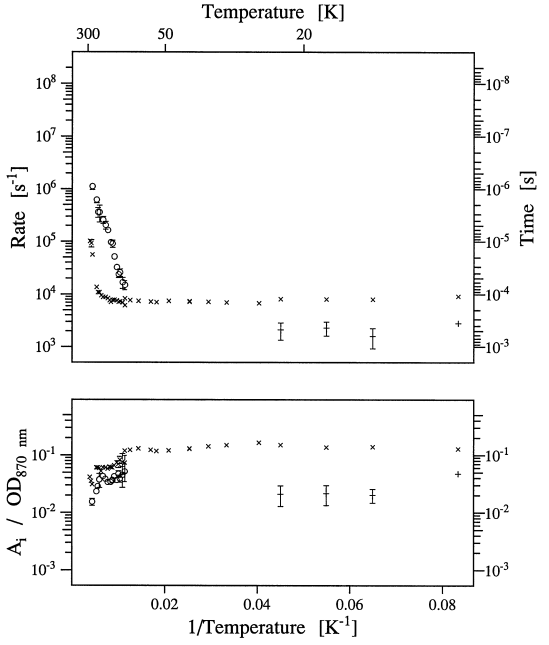

Fig. 7. Top: $^3P_{870}$ decay rates in *Rb. sphaeroides* R26.1, B_A and B_B exchanged with [3-vinyl]-13^2-OH-BChl *a* and reconstituted with spheroidene (sample C) in an Arrhenius plot. The transients were observed between 870 and 895 nm (depending on the location of the P_{870} maximum at different temperatures) in different time intervals and evaluated by either a mono- or a bi-exponential (below 25 and above 100 K) fit to the decay of the signal. Bottom: Amplitudes of the kinetic components normalized to the OD at the acquisition wavelength (between 870 and 895 nm) with corresponding symbols.

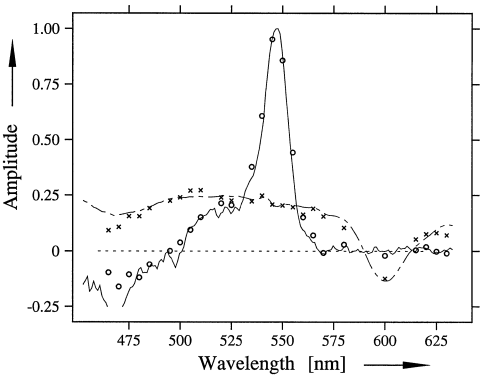

Fig. 8. Wavelength dependence of the amplitudes of the decay rates observed at 550 nm on the triplet–triplet absorption band of spheroidene in *Rb. sphaeroides* R26.1, B_A and B_B exchanged with [3-vinyl]-13^2-OH-BChl *a* and reconstituted with spheroidene (sample C) at 55 K. Open circles correspond to the ^{3}Car decay rate. The ×s correspond to the residual signal of the $^3P_{870}$ triplet–triplet absorption which appears as a slowly decaying component in the transients. The lines represent the MIA spectra of ^{3}Car (full line) and $^3P_{870}$ (broken line).

3.3. Transient spectra

For spectral identification of the observed kinetic components the transients were measured and analyzed between 450 and 650 nm. Fig. 8 displays the result for the ^{3}Car decay (○) in sample C at 55 K which had to be distinguished from the underlying triplet–triplet absorption of the longer lived $^3P_{870}$ (×). The two components compare very well with the microwave induced absorption (MIA) spectra

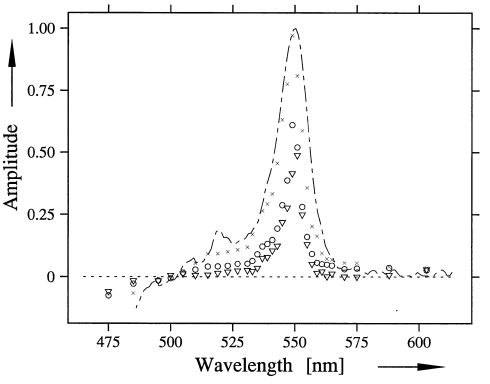

Fig. 9. Wavelength dependence of the amplitudes of the kinetic components observed at 550 nm on the triplet–triplet absorption band of spheroidene in *Rb. sphaeroides* R26.1, B_A exchanged with [3-vinyl]-13^2-OH-BChl *a* (sample B) at 45 K. ×, ^{3}Car decay rate; ○, fast rate of ^{3}Car formation (see Fig. 4); ▽, slow rate of ^{3}Car formation (see Fig. 4). The broken line represents the MIA spectrum of ^{3}Car.

of the two species. The MIA spectrum is a 'site-selective' triplet-minus-singlet spectrum that has been observed via the ADMR technique [38,58].

Fig. 9 shows the ^{3}Car decay as well as the two different ^{3}Car formation rates in comparison with its MIA spectrum for sample B. As can be seen, all observed rates follow the triplet-minus-singlet pattern of the ^{3}Car MIA spectrum and may be identified with the spheroidene triplet state. However, note the caveat for the fast rate as discussed below.

4. Discussion

4.1. Carotenoid triplet formation rates

As is evident from Figs. 3 and 4 the rise-time of the carotenoid triplet–triplet absorption signal is bi-exponential in the temperature range below about 100 K. Above 100 K the bi-exponentially persists in the B_B exchanged RCs while in samples with natural BChl *a* at B_B the two different rates seem to merge and are not distinguishable any more. The faster of the two rates shows a very weak temperature dependence (if any) and has a characteristic time constant between 10 and 100 ns. It may be due to radical-pair recombination kinetics, and may ultimately be limited by the time resolution in our experiment. A similarly fast component in the rise of the ^{3}Car triplet–triplet absorption signal was also observed by Kolaczkowski [1], and by Frank et al. [28].

The spectral response of this fast component is very similar to the spheroidene triplet-minus-singlet spectrum (see Fig. 9). This contrasts with the findings of Frank et al. [28] who observe a rather flat wavelength dependence of the temperature-independent fast rate which may perhaps be due to the wider spectral bandwidth used by these investigators and/or their noisier primary data.

The complication in the interpretation of the difference spectrum of the fast component is due to its similarity to the $^1[P^+_{870}H^-]$-minus-ground state difference spectrum [16], which makes $[P^+_{870}H^-]$ decay and ^{3}Car formation virtually indistinguishable in this spectral region. Of course, the transient due to $[P^+_{870}H^-]$ formation appears within 200 ps as a bleaching of the pheophytin absorption band at

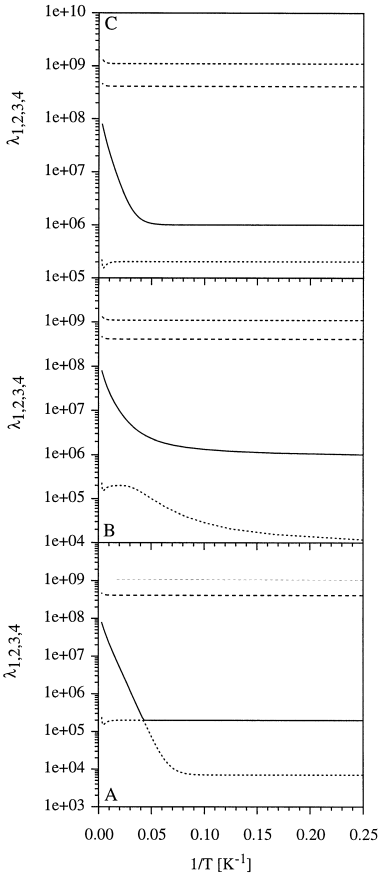

Fig. 10. Arrhenius plot of the calculated rates, i.e., the 4 kinetic components present in the 4-state model for the classic model (A), the classic model with heterogeneity (B), and the tunneling model (C) (see text and [40]).

546 nm and would be present during the laser pulse, while the ^{3}Car transient appears as an absorption increase. Thus the decay of $[P^+_{870}H^-]$ which takes place in the 10–50-ns range and the formation of ^{3}Car produce absorption changes in the same direction and in the same time window. We can therefore not exclude the possibility that part of the fast transient observed at 550 nm is due to $[P^+_{870}H^-]$ recombination.

The slow ^{3}Car formation rate which levels off at 1×10^6 s^{-1} does not suffer from this complication since $[P^+_{870}H^-]$ recombination occurs on a much faster time scale. Based on its spectral behavior it can clearly be interpreted as true ^{3}Car formation. The implications of this rate leveling off at 1×10^6 s^{-1} will be discussed below in conjunction with the $^3P_{870}$ decay.

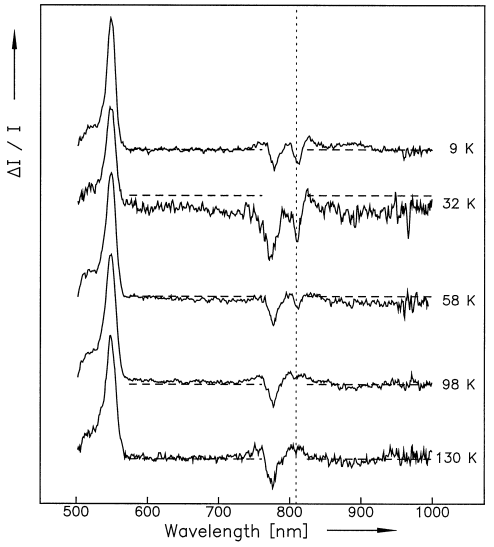

Fig. 11. MIA spectra of *Rb. sphaeroides* R26.1, B_A and B_B exchanged with [3-vinyl]-13^2-OH-BChl *a* and reconstituted with spheroidene (sample C) at 9, 32, 58, 98, and 130 K, observed on the $2|E|$ signal of the spheroidene triplet state. The spectra are normalized to equal height of the ^{3}Car triplet–triplet absorption peak at 550 nm. Microwaves were set at 267 MHz with 3 W power.

4.2. Primary donor bleaching decay rates

The temperature dependence of $^3P_{870}$ decay of sample B (RCs with B_A exchanged) is the richest in terms of observed exponentials (see Fig. 6). Apparently, the temperature independent components between 10 and 50 K observed with rates of approx. 10^6 s^{-1} and 10^7 s^{-1} resemble very well the observed ^{3}Car formation rates. While ^{3}Car does not have any known absorption components around 890 nm where the transients were observed it is theoretically expected that its rates show up in the kinetics of $^3P_{870}$ if both species can exchange energy [40]. Apparently, sample A (wild-type RCs) shows a similar behavior, although the onset at which these fast components can be distinguished from noise lies at higher temperatures (see Fig. 5). Sample C (both monomers exchanged) does not show any indication of these temperature independent fast rates (see Fig. 7). This may actually indicate that the fast temperature-independent rates observed at 550 nm in samples A and B are due to ^{3}Car formation rather than $[P^+_{870}H^-]$ decay since the latter is present in sample C as well while ^{3}Car formation is depressed at low temperature due to the higher triplet transfer barrier ^3B_B [28].

The rate that dominates $^3P_{870}$ decay for samples A and B is temperature dependent, rising from approx. 10^4 s^{-1} (above 30 K) to merge with the fast rates at higher temperatures. The slow (10^4 s^{-1}) rate observed at temperatures above 30 K with a thermally activated behavior above 100···150 K can be attributed to carotenoid-free RCs (see Section 3).

Table 2
Activation energies (in cm^{-1}) for $^3P_{870}$ decay, and ^{3}Car decay and formation

Sample	Activation energies in cm^{-1}	
	According to Eq. 5	According to Eq. 6
A: *Rb. sphaeroides* 2.4.1		
^{3}P870 decay	65 ± 10	95 ± 10
^{3}Car formation (fast)	105 ± 10	140 ± 15
^{3}Car formation (slow)	115 ± 10	195 ± 30
^{3}Car decay	32 ± 2	
B: *Rb. sphaeroides* 2.4.1 B_A exchanged		
$^3P_{870}$ decay	100 ± 5	105 ± 5
^{3}Car formation		110 ± 15
^{3}Car decay	35 ± 2	
C: *Rb. sphaeroides* R26.1 B_A, B_B exchanged, and reconstituted with spheroidene		
$^3P_{870}$ decay	410 ± 20	460 ± 20
^{3}Car formation (above 150 K)	310 ± 10	
^{3}Car decay	30 ± 3	

4.3. The slow ^{3}Car formation rate

The main question that we want to address in this section is: Why does the temperature dependent formation rate of the carotenoid triplet level off around 10^6 s^{-1} below 50 K? (Since sample C shows quite a different picture for $^3P_{870}$ decay than samples A and B, we defer the discussion of the B_B exchanged species to the next section.) This observation cannot only be seen in Figs. 3 and 4, but is also evident from previous reports [1,28,56]. While this kinetic rate is weakly observed in the $^3P_{870}$ decay as well (especially sample B, see Fig. 6), it does not correspond to the predominant $^3P_{870}$ decay rate at low temperatures. Kolaczkowski assumed a tunneling process to explain this rate which would only be observable at low temperatures when the thermally activated process shuts down [1].

Based on the linearized 4-level model described in Section 2 (for a detailed account see [40]) one can calculate the temperature dependence of the apparent rates observed on the transients of the triplet concentrations on the primary donor as well as on the carotenoid. These rates correspond to the inverse lifetimes of states 1–4 in the 4-level model (see Fig. 1). It is especially revealing to compare the results of the classical model (no tunneling, $k_{4\leftarrow2}$, and no bypass, $k_{3\leftarrow1}$, process assumed) with and without heterogeneity of the energy level of ^3B_B (see Fig. 10A,B) with the tunneling model (see Fig. 10C). All three models show two temperature-independent slow rates at low temperatures.

The question then is, whether it is possible to model a temperature independent rate at 1×10^6 s^{-1} for the carotenoid formation as observed in the experiment. Apparently, this is not possible for the classic model (without provision for tunneling, bypassing, or heterogeneity, Fig. 10A). At low temperatures the only slow rates observable are the inverse lifetimes of the primary donor and the carotenoid triplet (decay rates of 1×10^4 s^{-1} and 2×10^5 s^{-1}, respectively). Obviously, one would not even expect to observe ^{3}Car at all at temperatures low enough where the thermally activated triplet transfer becomes slower than the intrinsic lifetime of $^3P_{870}$ (the intensity of the 2×10^5 s^{-1} kinetic component would be too small to be observable). This rules out the classic model. It can also be rejected based on the observation of the presence of ^{3}Car at temperatures as low as 4.2 K with ODMR [29–31].

Kolaczkowski's assumption of a tunneling process that would only be visible at low temperatures when the thermally activated triplet transfer becomes inefficient [1] also does not solve the question. In this case it is of course possible to simulate an apparent rate of 1×10^6 s^{-1} by arbitrarily assuming it to be the tunneling rate $k_{4\leftarrow2}$ in the model (see Figs. 1 and 10C). However, this assumption excludes the observability of the intrinsic $^3P_{870}$ decay at all. Obviously, tunneling would dominate over the ISC decay of the primary donor triplet at low temperatures which would make it impossible to observe the dominant decay rate of 1×10^4 s^{-1} as seen in Figs. 5 and 6 which is comparable to carotenoid-free mutants. These kinetic components would only be observed from the minor contribution of carotenoid-free RCs whose intensities appear at least 1 order of magnitude below the intensity of the carotenoid-containing main component. One can see that this is not the case in Figs. 5 and 6. Rather the slow component attributed to $^3P_{870}$ decay dominates the amplitudes at low temperature. Furthermore, if tunneling were a valid route for triplet energy transfer from $^3P_{870}$ to ^{3}Car one would expect to observe high concentrations of ^{3}Car down to 4.2 K, e.g., by EPR, which is not the case [27].

The explanation which we would like to put forward introduces a heterogeneity of the energy level of ^3B_B. We assumed a Gaussian distribution of energy levels with a half width $\Gamma = 95$ cm^{-1}, which corresponds to the linewidth of the singlet ground state absorption spectrum of B_B [38]. As seen from Fig. 10B, the resulting simulation yields an apparent rate of the order of 1×10^6 s^{-1} at low temperatures in addition to the intrinsic $^3P_{870}$ decay of 1×10^4 s^{-1}. Obviously, the decay rates are not mono-exponential any more and the plotted rates are weighted averages of the expected theoretical rates as they would appear in the experiment. The distribution of rates now also results in non-linear dependencies on inverse temperature in the Arrhenius plot and complicates the analysis of the energy barrier. As the temperature is dropped, less and less RCs will participate in the triplet energy transfer process leaving only those at the low energy wing of the non-homogeneous distribution of ^3B_B energy levels to produce ^{3}Car. This

model not only explains the apparent temperature independent slow ^{3}Car formation rate at low temperatures but also the available magnetic resonance data. One would expect the ^{3}Car concentration to drop sharply around 30–40 K as observed in light-induced cw-EPR experiments [25]. On the other hand, low concentrations of ^{3}Car would still be observable down to very low temperatures, stemming from the fraction of RCs with very low ^3B_B energies relative to the primary donor triplet state. This would explain the observation of ^{3}Car ODMR signals down to 4.2 K [29–31]. Under many circumstances, ODMR is much more sensitive than cw-EPR and therefore might pick up very low triplet concentrations which would not show up in cw-EPR. Finally, this model might also explain the direct observation of ^3B_B by zero-field ADMR in carotenoid-free mutants of *Rb. sphaeroides* [59]. It should be in dynamic equilibrium with $^3P_{870}$ due to the close proximity of the two pigments. In the classic model all triplet energy would end up on $^3P_{870}$ and thus ^3B_B would not be observed by ODMR. However, with the assumption of heterogeneity of the energy of ^3B_B, and/or in $^3P_{870}$ for that matter, there would be a fraction of RCs in the sample that has ^3B_B lower in energy than $^3P_{870}$ thus rendering it observable. It should be added that of course the heterogeneity may also be present in the triplet energy level of the primary donor itself, $^3P_{870}$, which would also lead to the observed effects since only the relative energy difference between $^3P_{870}$ and ^3B_B has to change sign to observe activation-less triplet energy transfer from $^3P_{870}$ to ^3B_B.

Summarizing this section we want to stress that it is not necessary to invoke an unlikely tunneling process at low temperatures to explain the slow temperature independent carotenoid triplet formation process. Instead, it is possible to reconcile the transient optical data with previous magnetic resonance results by assuming heterogeneity in the energy level of ^3B_B (and/or $^3P_{870}$).

4.4. The fast ^{3}Car formation rate

Kolaczkowski showed evidence for the fast temperature independent process without backing it up with an absorption difference spectrum [1]. Frank et al. also observed a fast component but discounted it as due to primary donor triplet formation because its spectral shape lacked the characteristic peak around 550 nm [28]. Closer inspection of Fig. 5 in [28] shows a slight maximum around 545 nm that could perhaps in part be due to a spheroidene triplet–triplet absorption band. It may very well be that the lower signal-to-noise ratio in the original transients (compare Fig. 2a in [28] with our Fig. 2 top panel) combined with lower spectral resolution precluded these workers from resolving the ^{3}Car absorption peak in the spectrum of their fast rising component. Our absorption difference spectra (see Fig. 9) clearly show a peak at 550 nm for the fast kinetic component.

Nevertheless, due to the similarity of the carotenoid triplet–triplet absorption spectrum with the difference spectrum of $[P^+_{870}H^-]$ recovery it seems premature to speculate about a possible mechanism which could explain such a fast ^{3}Car formation in bypassing $^3P_{870}$ as proposed by Kolaczkowski [1].

4.5. The energy barrier, ^3B_B

The fact that we have to assume substantial heterogeneity (i.e., broadening) of the energy level of ^3B_B makes it difficult to obtain a good number for its value. For once, the thermally activated rate does not obey a strict Arrhenius behavior any more (as can be seen by the predicted curved lines in Fig. 10B). On the other hand, our data are still too noisy to use the extended model and to include the degree of heterogeneity as a free fit parameter. It therefore has to be kept in mind that the application of a strict Arrhenius law, and the energy barriers derived from it are fraught with a substantial uncertainty not only due to fitting errors but also due to the convolution of rates from different subpopulations of reaction centers. It is especially hazardous to take the thermal activation of the slow component of the ^{3}Car formation rate because at low temperatures only a subpopulation of RCs is sampled. Additionally, in the vinyl-BChl (B_B) exchanged sample C a certain percentage of unexchanged RCs is present [38,60], and may be the reason why the slopes of the slow ^{3}Car formation (above 100 K) in Fig. 4 and the rate of $^3P_{870}$ decay in Fig. 7 do not coincide with each other (see also further discussion below). We therefore prefer to take the rates from the temperature

dependence of the $^3P_{870}$ life-time since one always observes the bulk behavior in this case.

Table 2 shows the activation energies obtained for the different samples from the analysis of the temperature dependence of their $^3P_{870}$ decay, and ^{3}Car decay and formation rates. For ^{3}Car only the slow formation rate was used since it is due to the thermally activated energy transfer while the fast rate may be due to a bypass reaction for which no temperature dependence is expected, and may be obscured by or entirely due to $[P^+_{870}H^-]$ recombination.

The rates were fit to the Arrhenius equation

$$k_{\text{observed}} = k_0 \exp\left\{-\frac{\Delta E}{k_B T}\right\} \quad (5)$$

where k_0 corresponds to $k_{2\leftarrow 3}$ of the 4-state model (see Fig. 1), and k_{observed} is the observed rate of either $^3P_{870}$ decay (see Figs. 5–7), or ^{3}Car formation (see Fig. 3 or Fig. 4); k_B is Boltzmann's factor. Since the rates level out at low temperatures, only data points above 100 K (above 140 K for sample C) can be used for the fit as they provide approximately straight lines in the log k vs. $1/T$ plot.

In order to include more data points at lower temperatures and increase the accuracy of the fits we included the low temperature rates in the fits, by:

$$k_{\text{observed}} = k_{[^3P]} + k_0 \exp\left\{-\frac{\Delta E}{k_B T}\right\} \quad (6)$$

where $k_{[3P]}$ is the life-time of $^3P_{870}$ at very low temperatures (with no thermally activated energy transfer present).

If we take the evaluation of the $^3P_{870}$ decay with Eq. 6 as the most reliable figure for the energy barrier we arrive at a difference of approximately 360 cm^{-1} in activation energies between native BChl *a* and [3-vinyl]-13^2-OH-BChl *a* at B_B.

This is less than the energy difference of their singlet excited states (approx. 590 cm^{-1} [38]) which indicates slightly different exchange interactions in the LUMOs of the two molecules, or might be ascribed to the effect of heterogeneity that puts heavier weights on lower energy barriers in the experimental observation of triplet energy transfer (thus 'pulling down' the higher energy barrier more than the lower one).

Our results are consistent with those previously reported by Frank et al. [28]. The values for wild-type RCs match exactly if we compare our data from the analysis of the temperature dependent ^{3}Car formation (140 ± 15 cm^{-1}) with theirs (140 ± 100 cm^{-1}). For the afore-mentioned reasons we believe that the evaluation of the temperature dependence of the $^3P_{870}$ decay rates is more reliable. It leads to somewhat lower values of around 95 ± 10 cm^{-1}. This is still consistent with [28] considering the large error margin given, and our sample B (105 ± 5 cm^{-1}) as well as the values given by Kolaczkowski (130 ± 20 cm^{-1}) [1]. Work on RCs from *Rsp. rubrum* S1 found an energy barrier of 190 cm^{-1} [31] but in that case B_B appears to be slightly blue-shifted as compared to *Rb. sphaeroides* [60] which may explain the difference.

Sample C exhibits a discrepancy of the activation energies of about 100–150 cm^{-1} as measured from the temperature dependence of ^{3}Car formation and $^3P_{870}$ decay (see Table 2). Since we believe that this sample may be contaminated with small amounts of RCs not exchanged at B_B (see below) it is especially hazardous to take the ^{3}Car formation rate as a measure of triplet energy transfer. At low temperatures the contamination will contribute over-proportional due to its lower activation barrier. We therefore believe that the value of 460 ± 20 cm^{-1} is more accurate for the energy barrier in this case, of course with the cautionary remark that heterogeneity is expected to play a role in sample C, too. Since heterogeneity always tends to favor RCs with lower energy barriers in the observation of the transients, the real median value may actually still be higher. Our results are in agreement with those reported by Frank et al. [28] (380 ± 100 cm^{-1}) within their large error margin. However, these workers used the ^{3}Car population for their analysis which underestimates the true energy barrier.

4.6. The B_B exchanged sample C

Closer inspection of the ^{3}Car formation rates of the [3-vinyl]-13^2-OH-BChl *a* exchanged sample C (Fig. 4) shows a peculiar behavior of the slow component which in our view can only be explained by the heterogeneity in the sample composition (not the inherent heterogeneity in the energy of ^3B_B but the presence of unexchanged RCs). At low temperatures (below 100 K) the rate appears to rise steadily from

approx. 1×10^6 s^{-1} (at 20 K) to approx. 4×10^6 s^{-1} (around 100 K) in good agreement with the observation in wild-type RCs (filled circles). Above 100 K the rate apparently drops to slightly below 1×10^6 s^{-1}, and rises again with temperature with a much steeper slope to arrive at 4×10^6 at around 300 K. The slope translates into an activation energy of 310 ± 10 cm^{-1} (see Table 2).

The MIA spectra of the spheroidene triplet state in sample C (see Fig. 11) supplies us with a plausible explanation for this behavior. The BChl region shows two distinct bleaching bands in the low temperature spectra (9 K to 58 K) with maxima at 812 and 775 nm. At higher temperatures only the band at 775 nm persists. These bands can be ascribed to the partial bleaching of B_B while the spheroidene molecule is in its triplet state [38]. Clearly, at low temperatures we are picking up some fraction of RCs that have not been exchanged with [3-vinyl]-13^2-OH-BChl *a* at B_B thus exhibiting the native B_B bleaching at 812 nm. According to HPLC analysis this fraction is rather small, approx. 5% of the total population [38]. Nevertheless it produces a signal comparable in strength to the 95% of [3-vinyl]-13^2-OH-BChl *a* exchanged RCs at 9 K. The impurity is favored against the bulk due to the lower energy barrier for triplet energy transfer. The same is expected to happen in the transient absorption measurements, explaining why the slow rate of ^{3}Car formation of samples C and A are so similar below 100 K. Above 100 K the MIA signals are due to the bulk of [3-vinyl]-13^2-OH-BChl *a* exchanged RCs drowning out the impurity band at 812 nm. The ^{3}Car formation rates taken from the corresponding absorption transients reflect the triplet transfer activity of the modified RCs.

Finally, we want to point out that due to the contamination with non-exchanged RCs the application of the 4-state model to the ^{3}Car formation rates does not bring additional information. At low temperatures we would only get the results obtained from samples A and B because the contamination dominates the ^{3}Car formation. At higher temperatures a simple Arrhenius analysis suffices to extract the apparent energy barrier.

5. Conclusions

In this study we have analyzed carotenoid triplet formation and decay as well as primary donor triplet decay in RCs from *Rb. sphaeroides* 2.4.1 (wild-type, sample A), exchanged at position B_A with [3-vinyl]-13^2-OH-BChl *a* (sample B), and those from the mutant R26.1, exchanged at both monomer positions with [3-vinyl]-13^2-OH-BChl *a* and reconstituted with spheroidene. A simple model for triplet energy transfer was used to interpret the experimental data. We can explain the slow temperature independent ^{3}Car formation rate at low temperatures by introducing a heterogeneity in the energy of ^3B_B. A Gaussian distribution with a half width of 95 cm^{-1} simulates the observation rather well. The observation of an additional temperature independent fast kinetic component on both the ^{3}Car triplet–triplet absorption and the $^3P_{870}$ bleaching bands may be due to either an additional triplet transfer process bypassing the vibronically relaxed $^3P_{870}$, or may be explained by the $[P^+_{870}H^-]$ recombination kinetics. The quality of our data is not good enough to clearly distinguish between both possibilities.

The energy barriers for triplet energy transfer from $^3P_{870}$ to ^{3}Car via ^3B_B were estimated to be of the order of 100 ± 10 cm^{-1} for samples A and B where B_B has not been exchanged, and 460 ± 20 cm^{-1} for sample C where B_B has been exchanged against [3-vinyl]-13^2-OH-BChl *a*.

Acknowledgements

This work was supported by the Deutsche Forschungsgemeinschaft under contract Wo41/42-2, An160/6-1, and SFB 143, project A9. A.A. thanks Prof. H.C. Wolf for his continued support. We thank W. Schäfer (Max-Planck-Institut für Biochemie, Martinsried) for providing mass spectra, and E. Cmiel (Technische Universität, München) for NMR spectra of the modified pigments. We also thank C. Bubenzer for growing the bacteria, and I. Katheder for the pigment preparations. G.H. acknowledges a graduate scholarship of the 'Freistaat Bayern'.

References

[1] S.V. Kolaczkowski, On the Mechanism of Triplet Energy Transfer from the Triplet Primary Donor to Spheroidene in Photosynthetic Reaction Centers from *Rhodobacter sphaeroides* 2.4.1, Ph.D. thesis, Brown University, Providence, RI, 1989.

[2] D.W. Reed, G.A. Peters, J. Biol. Chem. 247 (1972) 7148–7152.

[3] S.C. Straley, W.W. Parson, D.C. Mauzerall, R.K. Clayton, Biochim. Biophys. Acta 305 (1973) 597–609.

[4] R.J. Cogdell, W.W. Parson, M.A. Kerr, Biochim. Biophys. Acta 430 (1976) 83–93.

[5] G. Feher, Photochem. Photobiol. 14 (1971) 373–387.

[6] M.Y. Okamura, L.A. Steiner, G. Feher, Biochemistry 13 (1974) 1394–1403.

[7] T.O. Yeates, H. Komiya, A. Chirino, D.C. Rees, J.P. Allen, G. Feher, Proc. Natl. Acad. Sci. USA 85 (1988) 7993–7997.

[8] C.-H. Chang, O. El-Kabbani, D. Tiede, J. Norris, M. Schiffer, Biochemistry 30 (1991) 5352–5360.

[9] U. Ermler, G. Fritzsch, S.K. Buchanan, H. Michel, Structure 2 (1994) 925–936.

[10] D. Siefermann-Harms, Physiol. Plant. 69 (1987) 561–568.

[11] R.J. Cogdell, H.A. Frank, Biochim. Biophys. Acta 895 (1987) 63–79.

[12] B. Andersson, A.H. Salter, I. Virgin, I. Vass, S. Styring, J. Photochem. Photobiol. B: Biol. 15 (1992) 15–31.

[13] R.J. Cogdell, T.G. Monger, W.W. Parson, Biochim. Biophys. Acta 408 (1975) 189–199.

[14] T.G. Monger, R.J. Cogdell, W.W. Parson, Biochim. Biophys. Acta 449 (1976) 136–153.

[15] C.C. Schenck, P. Mathis, M. Lutz, Photochem. Photobiol. 39 (1984) 407–417.

[16] V.A. Shuvalov, W.W. Parson, Proc. Natl. Acad. Sci. USA 78 (1981) 957–961.

[17] A.J. Hoff, I.I. Proskuryakov, Chem. Phys. Lett. 115 (1985) 303–310.

[18] E.J. Lous, A.J. Hoff, Photosyn. Res. 9 (1986) 89–101.

[19] I.I. Proskuryakov, K. Manikowsky, Dokl. Akad. Nauk SSSR 297 (1987) 1250–1252.

[20] V. Aust, A. Angerhofer, P.H. Parot, C.A. Violette, H.A. Frank, Chem. Phys. Lett. 173 (1990) 439–442.

[21] J. Ullrich, A. Angerhofer, J.U. von Schütz, H.C. Wolf, Trends Photochem. Photobiol. 1 (1990) 243–258.

[22] A. Angerhofer, R. Speer, J. Ullrich, J.U. von Schütz, H.C. Wolf, Appl. Magn. Res. 2 (1991) 203–216.

[23] L. Takiff, S.G. Boxer, Biochim. Biophys. Acta 932 (1988) 325–334.

[24] L. Takiff, S.G. Boxer, J. Am. Chem. Soc. 110 (1988) 4425–4426.

[25] H.A. Frank, C.A. Violette, Biochim. Biophys. Acta 976 (1989) 222–232.

[26] H.A. Frank, Trends Photochem. Photobiol. 1 (1990) 1–4.

[27] H.A. Frank, V. Chynwat, G. Hartwich, M. Meyer, I. Katheder, H. Scheer, Photosyn. Res. 37 (1993) 193–203.

[28] H.A. Frank, V. Chynwat, A. Posteraro, G. Hartwich, I. Simonin, H. Scheer, Photochem. Photobiol. 64 (1996) 823–831.

[29] J. Ullrich, R. Speer, J. Greis, J.U. von Schütz, H.C. Wolf, R.J. Cogdell, Chem. Phys. Lett. 155 (1989) 363–370.

[30] V. Aust, A. Angerhofer, J. Ullrich, J.U. von Schütz, H.C. Wolf, R.J. Cogdell, Chem. Phys. Lett. 181 (1991) 213–221.

[31] A. Angerhofer, V. Aust, U. Hofbauer, H.C. Wolf, in: N. Murata (Ed.), Research in Photosynthesis, Vol. 1, Kluwer Academic Publishers, Dordrecht, 1992, pp. 129–132.

[32] A. Müller, Pigmentaustausch und -Einbau in Photosynthetischen Reaktionszentren aus *Rhodopseudomonas viridis* und *Rhodobacter sphaeroides*, Ph.D. thesis, Universität München, 1992.

[33] A. Struck, A. Müller, H. Scheer, Biochim. Biophys. Acta 1060 (1991) 262–270.

[34] G. Feher, M.Y. Okamura, in R.K. Clayton, W.R. Sistrom (Eds.), The Photosynthetic Bacteria, Plenum Press, New York, NY, 1978, pp. 349–389.

[35] A. Struck, E. Cmiel, I. Katheder, W. Schäfer, H. Scheer, Biochim. Biophys. Acta 1101 (1992) 321–328.

[36] H. Scheer, A. Struck, in J. Deisenhofer, J.R. Norris (Eds.), The Photosynthetic Reaction Center, Vol. I, Academic Press, San Diego, CA, 1993, pp. 157–192.

[37] A. Struck, H. Scheer, FEBS Lett. 261 (1990) 385–388.

[38] G. Hartwich, H. Scheer, V. Aust, A. Angerhofer, Biochim. Biophys. Acta 1230 (1995) 97–113.

[39] A. Angerhofer, F. Bornhäuser, A. Gall, R.J. Cogdell, Chem. Phys. 194 (1995) 259–274.

[40] A. Angerhofer, Triplettzustände in Photosynthetischen Pigment–Protein Komplexen – Untersuchungen mit Optisch Nachgewiesener Resonanz und Doppelresonanz, Logos Verlag, Berlin, ISBN 3-931216-62-4, 1997.

[41] R. Speer, Zeitaufgelöste ADMR an Reaktionszentren Photosynthetisierender Bakterien, Diplomarbeit, Universität Stuttgart, 1988.

[42] S. Kolaczkowski, D. Budil, J.R. Norris, in J. Biggins (Ed.), Progress in Photosynthesis Research, Vol. I, Martinus Nijhoff, Dordrecht, 1987, pp. 2.213–2.216.

[43] A. Ogrodnik, M. Volk, R. Letterer, R. Feick, M.E. Michel-Beyerle, Biochim. Biophys. Acta 936 (1988) 361–371.

[44] C.E.D. Chidsey, C. Kirmaier, D. Holten, S.G. Boxer, Biochim. Biophys. Acta 766 (1984) 424–437.

[45] C.E.D. Chidsey, L. Takiff, R.A. Goldstein, S.G. Boxer, Proc. Natl. Acad. Sci. USA 82 (1985) 6850–6854.

[46] D.E. Budil, S.V. Kolaczkowski, J.R. Norris, in J. Biggins (Ed.), Progress in Photosynthesis Research, Vol. I, Martinus Nijhoff, Dordrecht, 1987, pp. 1.25–1.28.

[47] A. Ogrodnik, N. Remy-Richter, M.E. Michel-Beyerle, R. Feick, Chem. Phys. Lett. 135 (1987) 576–581.

[48] R.A. Goldstein, S.G. Boxer, Biochim. Biophys. Acta 977 (1989) 70–77.

[49] R.A. Goldstein, S.G. Boxer, Biochim. Biophys. Acta 977 (1989) 78–86.

[50] R.A. Goldstein, L. Takiff, S.G. Boxer, Biochim. Biophys. Acta 934 (1988) 253–263.

[51] S.G. Boxer, R.A. Goldstein, D.J. Lockhart, T.R. Middendorf, L. Takiff, J. Phys. Chem. 93 (1989) 8280–8294.
[52] M. Bixon, M.E. Michel-Beyerle, J. Jortner, Isr. J. Chem. 28 (1988) 155–168.
[53] M. Bixon, J. Jortner, M.E. Michel-Beyerle, Z. Phys. Chem. 180 (1993) 193–208.
[54] V.A. Shuvalov, W.W. Parson, Biochim. Biophys. Acta 638 (1981) 50–59.
[55] G.L. Closs, M.D. Johnson, J.R. Miller, P. Piotrowiak, J. Am. Chem. Soc. 111 (1989) 3751–3753.
[56] U. Hofbauer, Transiente Absorption an Carotinoid Triplettzuständen in Reaktionszentren Photosynthetisierender Bakterien, Diplomarbeit, Universität Stuttgart, 1992.
[57] A.J. Hoff, H.G. de Vries, Biochim. Biophys. Acta 503 (1978) 94–106.
[58] H.J. den Blanken, A.J. Hoff, Biochim. Biophys. Acta 681 (1982) 365–374.
[59] A. Angerhofer, V. Aust, J. Photochem. Photobiol. B: Biol. 20 (1993) 127–132.
[60] V. Aust, ADMR und Transiente Absorption zum Triplettenergietransfer im Bakteriellen Reaktionszentrum, Ph.D. thesis, Universität Stuttgart, 1995.